AMERICAN SOCIETY FOR MICROBIOLOGY | Applied and Environmental Microbiology

Novel Metal Cation Resistance Systems from Mutant Fitness Analysis of Denitrifying *Pseudomonas stutzeri*

Brian J. Vaccaro,[a] W. Andrew Lancaster,[a] Michael P. Thorgersen,[a] Grant M. Zane,[b] Adam D. Younkin,[b] Alexey E. Kazakov,[c] Kelly M. Wetmore,[c] Adam Deutschbauer,[c] Adam P. Arkin,[c] Pavel S. Novichkov,[c] Judy D. Wall,[b] Michael W. W. Adams[a]

Department of Biochemistry and Molecular Biology, University of Georgia, Athens, Georgia, USA[a]; Department of Biochemistry, University of Missouri, Columbia, Missouri, USA[b]; Environmental Genomics and Systems Biology Division, Lawrence Berkeley National Laboratory, Berkeley, California, USA[c]

ABSTRACT

Metal ion transport systems have been studied extensively, but the specificity of a given transporter is often unclear from amino acid sequence data alone. In this study, predicted Cu^{2+} and Zn^{2+} resistance systems in *Pseudomonas stutzeri* strain RCH2 are compared with those experimentally implicated in Cu^{2+} and Zn^{2+} resistance, as determined by using a DNA-barcoded transposon mutant library. Mutant fitness data obtained under denitrifying conditions are combined with regulon predictions to yield a much more comprehensive picture of Cu^{2+} and Zn^{2+} resistance in strain RCH2. The results not only considerably expand what is known about well-established metal ion exporters (CzcCBA, CzcD, and CusCBA) and their accessory proteins (CzcI and CusF), they also reveal that isolates with mutations in some predicted Cu^{2+} resistance systems do not show decreased fitness relative to the wild type when exposed to Cu^{2+}. In addition, new genes are identified that have no known connection to Zn^{2+} (*corB*, *corC*, Psest_3226, Psest_3322, and Psest_0618) or Cu^{2+} resistance (Mrp antiporter subunit gene, Psest_2850, and Psest_0584) but are crucial for resistance to these metal cations. Growth of individual deletion mutants lacking *corB*, *corC*, Psest_3226, or Psest_3322 confirmed the observed Zn-dependent phenotypes. Notably, to our knowledge, this is the first time a bacterial homolog of TMEM165, a human gene responsible for a congenital glycosylation disorder, has been deleted and the resulting strain characterized. Finally, the fitness values indicate Cu^{2+}- and Zn^{2+}-based inhibition of nitrite reductase and interference with molybdenum cofactor biosynthesis for nitrate reductase. These results extend the current understanding of Cu^{2+} and Zn^{2+} efflux and resistance and their effects on denitrifying metabolism.

IMPORTANCE

In this study, genome-wide mutant fitness data in *P. stutzeri* RCH2 combined with regulon predictions identify several proteins of unknown function that are involved in resisting zinc and copper toxicity. For zinc, these include a member of the UPF0016 protein family that was previously implicated in Ca^{2+}/H^{+} antiport and a human congenital glycosylation disorder, CorB and CorC, which were previously linked to Mg^{2+} transport, and Psest_3322 and Psest_0618, two proteins with no characterized homologs. Experiments using mutants lacking Psest_3226, Psest_3322, *corB*, *corC*, or *czcI* verified their proposed functions, which will enable future studies of these little-characterized zinc resistance determinants. Likewise, Psest_2850, annotated as an ion antiporter subunit, and the conserved hypothetical protein Psest_0584 are implicated in copper resistance. Physiological connections between previous studies and phenotypes presented here are discussed. Functional and mechanistic understanding of transport proteins improves the understanding of systems in which members of the same protein family, including those in humans, can have different functions.

The responses of microorganisms to metal toxicity have been well studied (1). In brief, metal ions can be toxic by binding to essential proteins or other molecules, causing them to become nonfunctional or function incorrectly. This occurs, for example, where the toxic metal ion binds to a binding site that requires a different metal ion to function. Toxic metal ions can also catalyze reactions that are detrimental to the cell, such as hydroxyl radical generation catalyzed by free iron ($Fe^{3+/2+}$) (2) or iron-sulfur cluster degradation by copper (3).

Understanding modes of toxicity and metal resistance systems is important, as the information gained from bacteria can be applied to human physiology and medicine. For example, Wilson's disease and Menkes disease are two human diseases caused by mutations in copper transporters (4). Likewise, acrodermatitis enteropathica, while less well-studied at a mechanistic level, is caused by a mutation of the SLC39A4 zinc transporter gene (5). Wilson's disease results in copper accumulation, which is known to cause tissue damage due to the generation of reactive oxygen species (4). Similarly, copper and zinc are known to be involved in neurodegenerative diseases, such as Alzheimer's and Parkinson's, again with a connection to oxidative stress, although their precise roles are still unclear (6). In addition, copper has long been used as

Received 17 June 2016 **Accepted** 27 July 2016

Accepted manuscript posted online 29 July 2016

Citation Vaccaro BJ, Lancaster WA, Thorgersen MP, Zane GM, Younkin AD, Kazakov AE, Wetmore KM, Deutschbauer A, Arkin AP, Novichkov PS, Wall JD, Adams MWW. 2016. Novel metal cation resistance systems from mutant fitness analysis of denitrifying *Pseudomonas stutzeri*. Appl Environ Microbiol 82:6046–6056. doi:10.1128/AEM.01845-16.

Editor: V. Müller, Goethe University Frankfurt am Main

Address correspondence to Michael W. W. Adams, adams@bmb.uga.edu.

Supplemental material for this article may be found at http://dx.doi.org/10.1128/AEM.01845-16.

an antimicrobial agent in agriculture, where the evolution of copper-resistant strains can cause problems for food production (7). Much of the current knowledge about the transport protein families and toxic effects relevant in each of these cases has been gained from studies in bacteria (8).

The resistance of microorganisms to potentially toxic metal ions generally involves decreasing the intracellular concentration of free metal ions through active transport to the periplasm or extracellular milieu (9) or sequestering metal ions in a tightly bound form (10). Several classes of transporters are involved, each with members that are specific for the removal of certain toxic metal ions (or groups of ions). In Gram-negative bacteria, metal resistance can be achieved through the expression of two separate systems. One transports metal ions across the plasma membrane, while the other transports them across the outer membrane (9, 11). Plasma membrane transporters are often P-type ATPase pumps (8) or members of the cation diffusion facilitator (CDF) protein family (e.g., CzcD, a Zn^{2+} transporter), driven by the proton motive force (12). The resistance-nodulation-division (RND) efflux pumps, named after the protein family of the A component (13), span the periplasm and are formed by proteins from the RND, membrane fusion protein (MFP), and outer membrane factor (OMF) families—the A, B, and C components, respectively (e.g., CzcCBA and CusCBA) (9, 14, 15). The RND protein is integrated in the cytoplasmic membrane, the MFP is in the periplasmic space, and the OMF is integrated in the outer membrane (13). Such transporters primarily serve to remove toxic metal ions from the periplasm. They can transport ions across both membranes, although this may be a signaling mechanism rather than a main transport pathway (9, 11, 13, 16). There are structural models for all three of these transporter classes (P-type ATPase, CDF, and RND type) available in the Protein Data Bank (13, 17, 18).

Generally, ion transporters or other metal-binding proteins are not absolutely specific in the metal ion or ions that they transport. For example, the CzcCBA (19) and CzcD (12) transporters are proposed to transport Co^{2+}, Zn^{2+}, and Cd^{2+}, and corresponding regulatory systems respond to these cations, as well as other metal ions in some cases (20–22). In addition, transporters that primarily import Mg^{2+} are a common source of various intracellular transition metals (23). Thus, transporters are not perfectly specific, due to similarities in the size, charge, and to some extent, coordination preferences of metal ions, particularly among the divalent late d-block metals (Fe-Zn). In some cases, lower-specificity transporters may even provide a competitive advantage (24, 25). However, the specificity (or generality) of a given transporter is currently very difficult to determine bioinformatically. For example, the InterPro protein family that contains *czcA* (IPR004763) contains RND proteins that are involved in the transport of any metal cation (26).

While bacteria frequently have several hundred or even a thousand transporter genes (14), in many cases, it is still unclear from sequence information alone which species each of them transports. Even transporters for organic molecules can be quite similar to metal ion transporters (15). Thus, gene annotations are often vague, and recognized protein families often include transporters of many different chemical species (IPR004763) or, sometimes, a very small collection of proteins for which the transported species is known (IPR005695) (26). In the case of copper and zinc, Cu^{2+} and Zn^{2+} are physically similar, but they have very different functions in cellular metabolism and are treated differently by transporters, since Cu^{2+} is readily reduced to Cu^{+} in the cytoplasm but Zn^{2+} is not redox active in the biological range (27). The transport of these ions has both agricultural and medical relevance (see above) and is the focus of this study.

Pseudomonas stutzeri is a model denitrifying gammaproteobacterium (28). Strain RCH2 was isolated from Hanford, a U.S. Department of Energy (DOE) Superfund site with metal contamination, particularly chromium, from a retired nuclear reactor complex (29). Strain RCH2 was originally characterized for its chromate-reducing activity (29), and a random barcode transposon site sequencing (RB-TnSeq) library is now available (30). In this study, we used this library to determine which RCH2 efflux systems were truly involved in Cu^{2+} and Zn^{2+} resistance during denitrifying growth (24). Since some Zn^{2+} transport systems can also transport Co^{2+} and Cd^{2+} (14), RB-TnSeq analysis was also conducted in the presence of toxic concentrations of each of these two metal ions for comparison. This work both extends results from well-characterized metal-resistant bacteria like *Cupriavidus metallidurans* (14) to test their generality and discovers some new determinants of metal resistance (14).

The RB-TnSeq technique provides a way to quantitatively measure, by multiplexed short-read DNA sequencing, the fitness of hundreds of thousands of single-insertion transposon mutant strains simultaneously (30). Fitness is measured by the abundance of an individual mutant relative to the overall mutant library population. The fitness values for mutants with insertions in the same gene are averaged to yield gene fitness values for nearly every gene in the genome. While single gene insertions may not always result in low fitness under conditions that make use of that gene, due to genetic redundancy (such as the presence of a paralog), the genome-wide fitness survey that is obtained can still reveal many key players in a given process. We grew the RCH2 RB-TnSeq library anaerobically with nitrate as the terminal electron acceptor and with and without the addition of toxic levels of Zn^{2+}, Cu^{2+}, Co^{2+}, or Cd^{2+}. Fitness values were assigned to 3,315 coding genes (out of 4,265 in the 4.6-Mb genome) (30) via parallel sequencing of strain barcodes. Certain genes that resulted in Zn^{2+}-sensitive phenotypes were also selected for the construction of individual deletion strains to confirm the phenotypes observed via the RB-TnSeq library and to enable further study.

MATERIALS AND METHODS

Growth screens. *P. stutzeri* RCH2 was cultured anaerobically in 100-well plates as previously described (24). Lactate (20 mM) was used as a carbon source, with nitrate (20 mM) as the terminal electron acceptor. The medium also contained 4.7 mM ammonium chloride, 1.3 mM potassium chloride, 2 mM magnesium sulfate, 0.1 mM calcium chloride, 0.3 mM sodium chloride, 29.7 mM sodium bicarbonate, and 5 mM sodium dihydrogen phosphate. Vitamins and minerals were added as described by Widdel and Bak (31). The medium was supplemented with various concentrations (1 to 1,500 μM) of $ZnCl_2$, $CuCl_2$, $CoCl_2$, or $CdCl_2$ to determine the concentration which yielded about 50% maximum optical density (OD) in 8 to 12 h compared to the OD of the untreated control.

Mutant library growth. The *P. stutzeri* RCH2 RB-TnSeq mutant library, containing 166,448 single transposon insertions with known, sequence-identified genome locations (30), was grown as previously described with nitrate (20 mM) as the electron acceptor (24). Zn^{2+}, Cu^{2+}, Co^{2+}, or Cd^{2+} toxicity was induced by supplementing the growth medium with 500 μM $ZnCl_2$, 100 μM $CuCl_2$, 100 μM $CoCl_2$, or 6 μM $CdCl_2$. Yeast extract (0.5 g/liter) was added in all cases to avoid eliminating insertion mutants from the population due to nutrient auxotrophy. The

addition of yeast extract also enhances growth, which expands the possible dynamic range of fitness values.

DNA isolation, PCR, sequencing, and sequence analysis. Sample processing, DNA sequencing, and analysis of sequence data were conducted as described previously; however, DNA samples were processed only by the BarSeq98 method (30). The PCR products were sequenced using the Illumina HiSeq system. Strain fitness values were calculated for each individual transposon insertion strain. Fitness is defined as the binary logarithm of the ratio of postgrowth and pregrowth relative abundances for that strain. Gene fitness values (w) were calculated, as previously described (30), by averaging the fitness values for strains with insertions in a given gene. The full set of gene fitness values, including values for each replicate, is reported in Table S1 in the supplemental material. Quality control and normalization of data were performed as previously reported (30), with only data from the sequencing runs mentioned here. Quality metrics for the fitness data are reported per growth condition in Table S2.

Generation of individual mutant strains. The construction of the deletion mutation strains used in this study (see Table S3 in the supplemental material) was accomplished by conjugating an unstable marker exchange plasmid (see Table S3) into *P. stutzeri* RCH2. Each plasmid was constructed by assembling either two or four PCR products together in α-select cells (Bioline) by the sequence- and ligation-independent cloning (SLIC) technique (32). These PCR products were amplified with *Herculase II* DNA polymerase (Stratagene) with primers (see Table S4) obtained from Integrated DNA Technologies. Each SLIC assembly reaction mixture contained a PCR product that included the plasmid backbone (spectinomycin resistance gene, pUC origin of replication, and origin of transfer), a PCR product containing a kanamycin resistance gene, and two PCR products flanking the gene to be deleted. For three of the marker exchange plasmids (plasmids for the deletion of the Psest_3322, Psest_0529, and Psest_3136 genes), the kanamycin resistance gene and the two homologous regions flanking the gene of interest were joined by sequence overlap extension (33) prior to the SLIC reaction. The PCR products of chromosomal regions flanking the gene to be deleted were the locations for double homologous recombination to exchange the gene of interest with the kanamycin resistance gene, *npt*. These PCR products were sequenced at the DNA core facility at the University of Missouri, Columbia, and compared with the published sequence for RCH2. The constructed mutagenic plasmid was then isolated and transformed into an *Escherichia coli* strain (WM3064) expressing the transfer function of RP4 (34), containing a *dapA* deletion, and capable of conjugation with RCH2. Following conjugation (35), RCH2 exconjugants were selected with 50 μg kanamycin/ml. Putative exconjugants were initially screened to check their sensitivity to spectinomycin (100 μg/ml) so that no kanamycin-resistant isolates containing the targeted gene (resulting from a single recombination event and therefore containing the spectinomycin resistance gene) were carried forward. The spectinomycin-sensitive isolates were further confirmed by Southern blotting to determine the presence or absence of the gene. After growth to early stationary phase, all strains were frozen in a 10% (vol/vol) glycerol solution. All *E. coli* cultures were grown in SOC or LC medium (36). When appropriate, diamino-pimelic acid (0.1 mM) was added to permit the growth of *E. coli* WM3064-derived strains.

Zinc sensitivity of individual mutant strains. Individual mutant strains and wild-type RCH2 were grown under the same conditions as the mutant library and with and without 1 mM $ZnCl_2$ to verify Zn^{2+}-sensitive phenotypes. Growth was monitored with a Bioscreen-C automated growth curve analysis system enclosed in a Plas-Labs La Petite anaerobic glove box under an argon atmosphere with <5% hydrogen for catalytic removal of oxygen.

Regulatory motif reconstruction and regulon prediction. Known target genes *czcC*, *cueA*, and *copA* for the respective metal-responsive regulatory systems CzcRS (37), CueR (38), and CopRS (39) were used as starting points for the identification of transcription factor (TF) binding motifs. We used the RegPredict Web server (40) for motif reconstruction. Sets of sequences upstream from *czcC*, *cueA*, and *copA2* orthologs (from −400 to +50 with respect to the translation start site) from *Pseudomonas* species genomes were selected, and a common motif with the highest information content was identified in each set with the "Discover profiles" tool of the RegPredict Web server. These motifs were used as position-weight matrices for the reconstruction of regulons in the Genome-Explorer software package (41). Briefly, a position-weight matrix was used for a whole-genome search in the upstream regions of coding genes (from −400 to +50 with respect to the translation start site), with a threshold equal to a minimal score among all sites in a training set of the matrix.

RESULTS AND DISCUSSION

Experimental approach and analysis of RB-TnSeq fitness data. The RCH2 mutant library was grown anaerobically, with lactate (20 mM) as the carbon source and electron donor and with nitrate (20 mM) as the electron acceptor. Toxic concentrations of Cu^{2+} (100 μM), Zn^{2+} (500 μM), Co^{2+} (100 μM), or Cd^{2+} (6 μM), which give approximately 50% growth inhibition, were added to this control medium, and cells from all conditions were analyzed with the RB-TnSeq technique. The focus of this study was to identify genes crucial for Cu^{2+} and Zn^{2+} resistance under denitrifying conditions. Co^{2+} and Cd^{2+} data were included where relevant to Zn^{2+} transport.

As previously described (24), the data are presented as gene fitness values (w), which reflect the growth of mutants with disruptions of individual genes relative to the overall mutant library population such that an increase in the relative abundance of mutants in which a gene is mutated shows positive fitness for that gene and a decrease shows negative fitness (30). Gene fitness values are interpreted as the effect of the absence of the gene product; however, in some cases, transposon insertion can affect the expression of downstream genes as well (so-called "polar effects") (42). The original report of the *P. stutzeri* strain RCH2 RB-TnSeq library included analyses of the influence of polar effects on the data and concluded that they did not have a major influence (30). A major contributing factor to this is that only data from insertion strains in which the insertion occurs within the central 80% of the gene are used. In addition, Table S5 in the supplemental material gives a per-gene analysis of whether polar effects may influence the data and conclusions discussed here. Gene fitness values for growth in the control medium are designated w_{ctrl}, and w_{ctrl} values are subtracted from gene fitness values for growth in the presence of a toxic metal to obtain corrected fitness values that only reflect changes in fitness due to the metal stress. Hence, "w_{Zn}" is used to describe gene fitness values for growth in medium with Zn^{2+} that have been corrected by the w_{ctrl} value. Likewise, "w_{Cu}," "w_{Co}," and "w_{Cd}" refer to values for gene fitness in medium supplemented with Cu^{2+}, Co^{2+}, or Cd^{2+}, respectively, that have had w_{ctrl} subtracted to isolate the effect due to the added metal ion. The Zn^{2+} and Cu^{2+} RB-TnSeq studies produced phenotypes over similar ranges ($-3.8 < w_{Zn} < 1.9$ and $-3.2 < w_{Cu} < 2.5$) and with similar standard deviations (0.36 and 0.33, respectively). There were 72 genes with $|w_{Zn}|$ values of >1 (see Table S6) and 56 genes with $|w_{Cu}|$ values of >1 (see Table S7).

Zinc toxicity. (i) The CzcICBA efflux system. The most severe w_{Zn} values for genes previously known to be involved in Zn^{2+} transport were observed for the genes encoding an RND-type transporter, *czcCBA* (Psest_0614 to Psest_0616), and a gene that has been observed in gene clusters with *czcCBA* (43), *czcI* (Psest_0613) (w_{Zn} values of -3.6 ± 0.1 [mean ± standard deviation]) (Fig. 1). There are three *czcCBA* homologs present in the

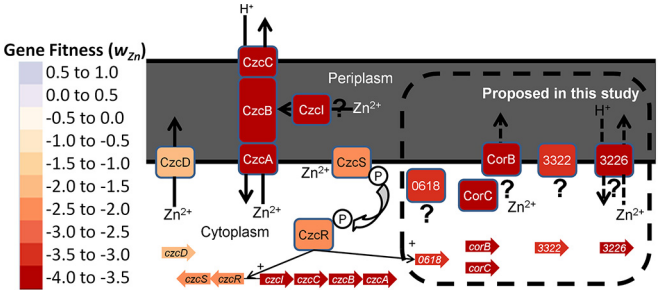

FIG 1 Zinc efflux in *Pseudomonas stutzeri* RCH2. Genes are represented by colored arrows at the bottom, and the proteins that they encode by boxes at their predicted cellular locations, labeled with Psest numbers where no name has been assigned. Bold arrows show ion transport, and thin arrows show gene regulation. Fitness values (w_{Zn}) are shown by the color scheme at left. Genes with previously recognized roles are shown on the left, and genes implicated in zinc resistance by the data presented here are shown in the dashed box on the right.

RCH2 genome, bearing the same UniProt annotation (Psest_1614 to Psest_1616, Psest_2265 to Psest_2263, and Psest_0598 to Psest_0596) (44). In order to determine how well annotations are likely to correspond to the specific ion that is transported, we generated a phylogenetic tree of the 4,253 sequences in the InterPro protein family (IPR004763), which contains CzcA and other RND family metal ion transporters (26). The set of proteins that bear annotations containing "copper," "Cu," or "cusA" was compared with those annotated by "zinc," "Zn," or "czcA," but not "family" (see Fig. S1 in the supplemental material). Annotations including "family" tended to be scattered across the phylogenetic tree. For additional categorization, the ScanProsite tool was used to search these sequences for motifs established by Nies for CzcA/CnrA versus CusA subfamilies (see Fig. S1) (9, 45). This analysis showed that the Nies motifs cluster proteins according to clades on the tree, whereas annotations correspond only weakly to phylogenetic clustering, lending confidence to Nies' assignments. Nies' motifs also correctly assigned CzcCBA from strain RCH2 as a divalent cation transporter. We are unaware of any similar test of Nies' predictions against phylogeny.

Although *czcICBA* are named for the ability to transport Co^{2+}, Zn^{2+}, and Cd^{2+}, the w_{Zn} values for these genes in strain RCH2 were 2.8 lower than the w_{Co} values (−0.8). These four genes are among the 8 genes with the most negative w_{Zn} values but are only among the 89 genes with the most negative w_{Co} values. All *czc* genes had w_{Cd} values between 0 and 0.2, so the CzcCBA system is not required for Cd^{2+} detoxification in RCH2 under denitrifying conditions. This could be due in part to the Zn^{2+} specificity of CzcS (46). However, the w_{Zn} values for *czcRS* were higher than those of the transporter genes (see Table S6 in the supplemental material), so it more likely reflects an altered specificity of the transporter from RCH2 relative to the specificities of other characterized CzcCBA transporters. It should be noted that the Cd^{2+} concentration used (for 50% growth inhibition) was only 6 μM, compared with 500 μM for Zn^{2+}. There was no analogous transport system encoded by genes with w_{Cd} values of less than −1. The effects of *czc* genes on Zn^{2+}, Co^{2+}, and Cd^{2+} resistance in *C. metallidurans* have been studied extensively (43).

The *czcI* gene is not widely distributed in nature, occurring in only 127 sequences, predominantly betaproteobacterial (IPR020487) (26). The true family is likely to be larger, as a BLAST search based on CzcI from strain RCH2 ($E < 10^{-10}$) identifies similar-length homologs with no InterPro match, and a few of them were included in IPR021333 (DUF2946). The CzcI protein is uncharacterized, and CzcCBA transporters are known to function in its absence (47). However, the negative w_{Zn} value for *czcI* observed in this study (−3.7) indicates that CzcI is an important component of the CzcCBA transporter in strain RCH2 (Fig. 1). It is predicted to localize to the periplasm and, thus, may play a role analogous to that of CusF, a periplasmic component of some CusCBA transport systems that is proposed to bind Cu^+ and promote its efflux through CusCBA (13). The somewhat sporadic taxonomic distribution of *czcI* among organisms often isolated from contaminated environments, combined with its relatively rare occurrence (26), suggests that it is a marker for high zinc resistance and is spread via horizontal gene transfer.

(ii) The CzcRS regulon. Homologs to the *czcSR* genes (Psest_0610 and Psest_0611), which are associated with CzcCBA regulation in *Pseudomonas aeruginosa* (37), also had negative w_{Zn} values (−2.2 ± 0.1). The CzcR DNA binding motif had not been described previously in *Pseudomonas* species, so we identified it in upstream regions of divergent *czcRS* and *czcCBA* operons from *P. aeruginosa*, *P. mendocina*, *P. syringae*, and *P. fluorescens*. A conserved 38-bp imperfect inverted repeat was found in all the sequences and is a candidate CzcR binding motif (see Fig. S2 in the supplemental material). We used this motif for a whole-genome search in *P. stutzeri* RCH2 and found five occurrences. Putative CzcR binding sites were predicted in an upstream region common to the *czcICBA* operon and the divergent Psest_0612 gene, encoding an outer membrane porin, indicating CzcRS-dependent expression of *czcICBA* in strain RCH2. Another binding site was identified upstream from the *czcRS* operon, suggesting autoregulation. The final two putative CzcR binding sites were found in an upstream region common to two divergent genes, Psest_0618 and Psest_0619. Psest_0618 encodes a hypothetical protein, whereas Psest_0619 encodes a CDF family transporter. Although the fitness data indicate that Psest_0619 is not required for Zn^{2+} resistance (w_{Zn} value of −0.1), regulon reconstruction indicates that it may be a redundant Zn^{2+} (or other metal ion) efflux pump. The number of sequencing reads for the two strains with Psest_0618 mutations was too low to assign a confident w_{Zn} value; however, the results do indicate strong Zn^{2+} sensitivity (w_{Zn} value of approximately −3), implicating this hypothetical protein in Zn^{2+} resistance (Fig. 1) and as a likely contributor to *czcRS* fitness, along with *czcICBA*. Close homologs to Psest_0618 are only found in *Pseudomonas* species, except for one close homolog (BLAST value, $E < 10^{-27}$) in *Streptococcus pneumoniae* (UniProt accession number A0A0T8LNT2) (44).

(iii) The CDF family CzcD transporter. Members of the CDF family of cation/proton antiporters export metal ions into the periplasm. The CDF InterPro family (IPR002524) contains nearly 35,000 sequences with wide sequence variety, such that it is particularly difficult to subcategorize them bioinformatically in terms of metal ion specificity (26). RCH2 contains a total of six such CDF proteins, but only one of these (Psest_2759), which we refer to as CzcD after the established convention (12), was encoded by a gene with a negative w_{Zn} value (−2.0). While a remote location of *czcD* relative to the position of *czcICBA* is not very surprising due to its functional independence, other homologs located quite close to the *czcICBA* operon, Psest_0607 (w_{Zn} of 0.0) and Psest_0619 (see above), would appear to be Zn^{2+} related *a priori*. Values of −0.2 for w_{Co} and 0.3 for w_{Cd} were observed for

Psest_2759, suggesting that the gene product is predominantly involved in Zn^{2+} tolerance. The positive w_{Cd} values for *czcICBA* and *czcD* may result from higher intracellular Zn^{2+} levels in the mutants, since Zn^{2+} can compete for binding sites that are targets for Cd^{2+} toxicity.

(iv) Hypothetical and poorly characterized proteins. In addition to genes predicted and annotated as part of transport systems, there were genes predicted to encode membrane-bound hypothetical proteins that resulted in strongly negative metal-specific phenotypes. These included Psest_3226, which had the second lowest w_{Zn} value (−3.7) (Fig. 1). Homologs of this gene can be found in all three domains of life. Defects in the human homolog have recently been shown to cause a newly discovered congenital glycosylation disorder (48). Subsequent patch clamp studies in human cells and phenotypic studies in yeast (49, 50) indicate that the protein functions as a H^+/Ca^{2+} antiporter, although no bacterial homologs have been characterized. According to the domain-based classification previously proposed, Psest_3226 from strain RCH2 is clearly a fusion of two UPF0016-type domains, as is found in eukaryotes, including two of the consensus EΨGDKT motifs (Ψ is most often I, L, or M) (50–52). The results presented here indicate that some proteins in this family can transport Zn^{2+} and, likely, other types of metal ions as well. The fitness values indicate that Psest_3226 is the primary Zn^{2+} efflux pump in the plasma membrane in strain RCH2, which should encourage further study of this protein in the future.

Another hypothetical membrane protein encoded by a gene with a high negative w_{Zn} value (−3.2) is Psest_3322 (Fig. 1). This large (138-kDa) protein belongs to the IPR011836 family of CHP02099 conserved hypothetical proteins, with homologs in the gamma- and betaproteobacteria, and contains a DUF3971 domain (IPR025263). It generally occurs in a six-gene operon, as in RCH2, encoding a predicted zinc-dependent protease (Psest_3320), an aminohydrolase (Psest_3321), an Rne/Rng family RNase (Psest_3323), and a septum formation inhibitor (Psest_3324). The other operon members did not result in significant phenotypes under the conditions tested, except for Psest_3323 (w_{Zn} of −1.0). Although the specific function of the protein encoded by Psest_3322 is not quite clear, it is apparently required for Zn^{2+} resistance. This phenotype could serve as a starting point for elucidating the function of this uncharacterized protein family.

Psest_3341 also had a high negative w_{Zn} value (−1.3). The protein encoded by this gene is a member of the large family of outer membrane TonB-dependent receptors and is likely involved in high-affinity siderophore-bound Fe^{3+} uptake, suggesting that Zn^{2+} toxicity is due in part to interference with iron uptake and metabolism. Mutation of this transporter likely eliminates a means of highly selective Fe^{3+} uptake, thus forcing the cell to rely on other means (that may leak more Zn^{2+}) or, possibly, to reduce the intracellular iron concentration such that Zn^{2+} can more effectively compete for Fe^{2+} binding sites.

(v) CorB and CorC. Three *Salmonella* genes were previously designated *corB*, *corC*, and *corD* because mutation of these genes led to enhanced Co^{2+} resistance (53), as did disruption of *corA*, which encodes a well-studied Mg^{2+} channel (54). The *corB* and *corC* homologs in strain RCH2 are remote from each other in the genome (Psest_3136 and Psest_0529) but exhibit strong cofitness (0.78), a measure of fitness correlation (55, 56), over many growth conditions (30), and they had very negative w_{Zn} values (−3.5 and −3.6, respectively) (Fig. 1). In *Salmonella*, CorBCD were proposed to enhance Mg^{2+} efflux through CorA (53). Strain RCH2 does contain homologs of *corA* (Psest_2314) and *corD* (Psest_3669); however, neither resulted in a significant phenotype under Cu^{2+} or Zn^{2+} toxicity conditions in strain RCH2. Hence, we propose that in strain RCH2, CorB and CorC work together, based on their high cofitness, but independently of CorA or CorD. Furthermore, CorB and CorC appear to function in Zn^{2+} efflux in strain RCH2 (Fig. 1). No results relating to Zn^{2+} efflux have been reported previously for these proteins, as they were thought to have a role only in efflux of Mg^{2+} (53). Assigning a role for CorB and CorC in CorA-independent efflux, however, leaves open the question of why *corB* and *corC* mutants have increased cobalt resistance (53). We believe this to be connected to CorA. If CorBC function in Mg^{2+} efflux under the conditions of wild-type Mg^{2+} efflux, the *corB* or *corC* deletion mutants would likely have elevated intracellular Mg^{2+} due to entry through the CorA Mg^{2+} channel. Elevated intracellular Mg^{2+} could cause enhanced Co^{2+} resistance, because Mg^{2+} enzymes are known intracellular targets of Co^{2+} toxicity (53, 57). The higher K_m of Co^{2+} import observed in the mutants (53) could likewise result from inhibition due to high intracellular Mg^{2+} favoring an inward-facing Mg^{2+}-bound conformation, thus reducing the effective enzyme concentration like a competitive inhibitor. It has long been believed that CorA itself mediates Mg^{2+} efflux, as well as uptake (54, 58). According to our reasoning, CorA is unlikely to be involved in efflux. Lack of Mg^{2+} efflux in the *Salmonella enterica corA* mutant (58) could occur simply because without CorA, intracellular Mg^{2+} does not reach concentrations high enough to induce efflux through CorBC. In addition, the presence of the CorA protein has regulatory effects in *S. enterica* that are not well understood, which would cause unanticipated effects in the *corA* mutant (59).

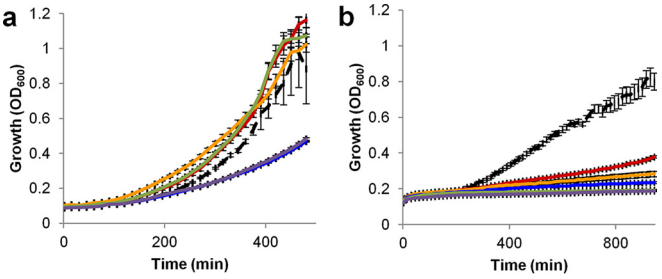

FIG 2 Growth of individual zinc-sensitive deletion mutants. Wild-type strain RCH2 is shown with a black trace, and mutant strains are shown in colors, as follows: Psest_3226 mutant is in red, *corC* mutant in yellow, *corB* mutant in blue, *czcI* mutant in green, and Psest_3322 mutant in purple. (a) Growth in control medium. (b) Growth in medium with 1 mM $ZnCl_2$ added.

(vi) Individual deletion mutants. Independent confirmation of the phenotypes observed in the RB-TnSeq experiments was obtained via the construction of individual deletion mutants for several poorly characterized or conserved hypothetical genes that were shown in the present work to be involved in Zn^{2+} resistance; namely, *czcI*, Psest_3226, Psest_3322, *corB*, and *corC*. Individual deletion mutants were constructed for each of these genes and, as shown by the results in Fig. 2, each strain was much more sensitive than the wild-type strain to growth inhibition by Zn^{2+}. For *czcI* in particular, these confirmatory results reduce the likelihood that the negative w_{Zn} value that was observed was due to polar effects of transposon insertions (see Table S5 in the supplemental material), although it is still possible that the genetic changes in the *czcI*

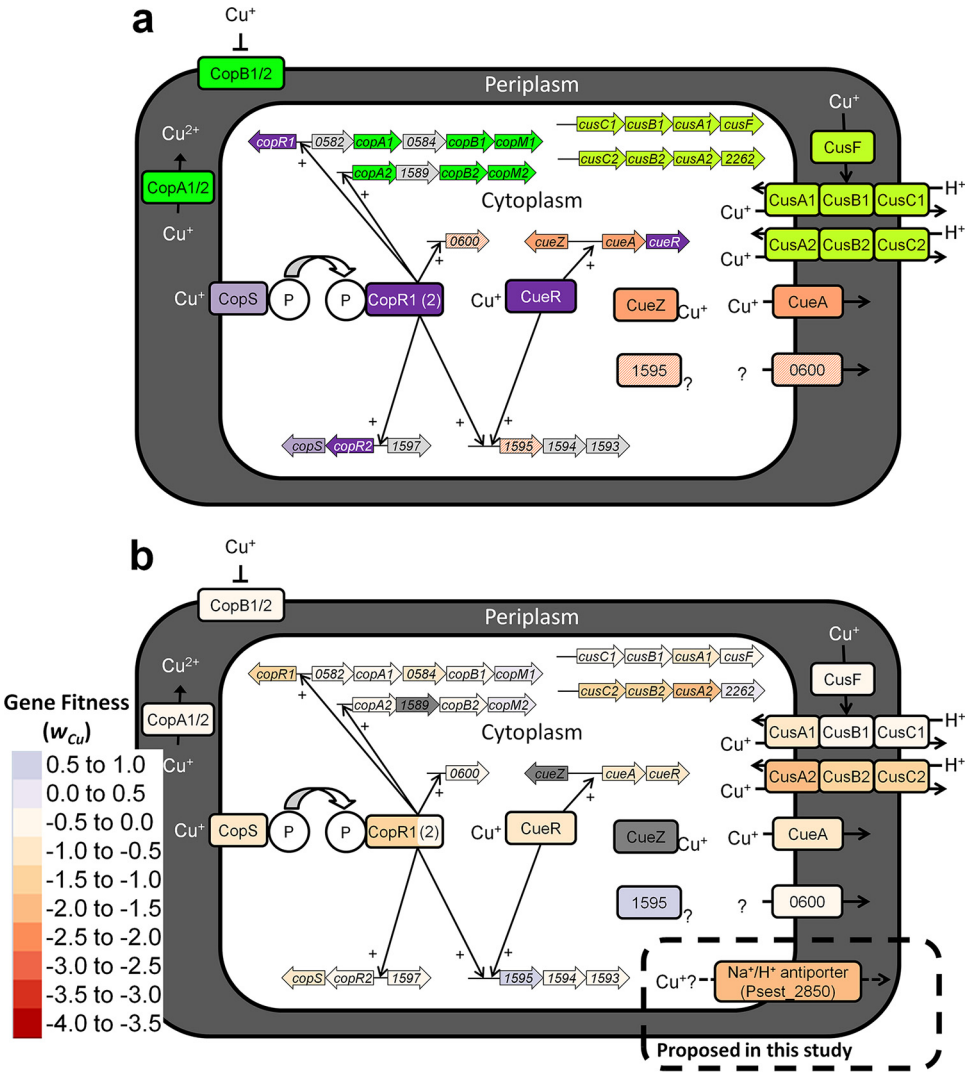

FIG 3 Copper efflux in *Pseudomonas stutzeri* RCH2. Genes are represented by colored arrows, and the proteins that they encode by boxes at their predicted cellular locations. Bold arrows show ion transport, and thin arrows show predicted gene regulation. (a) Colors correspond to functional classes or efflux systems (Psest_0600 and Psest_1595 are remote CueA and CueZ homologs with predicted copper regulation). Transcriptional regulators are shown in purple, and the copper sensor is shown in light purple. Proteins of unknown function are shown in gray. (b) Colors show fitness values (w_{Cu}) for the corresponding genes/encoded proteins according to the color scheme at left. Dark gray indicates insufficient data to assign a confident value. The gene implicated in copper resistance by the data presented here is shown in the dashed box on the right.

mutant could influence the expression of the *czcCBA* genes downstream. Further study of these mutants and of novel factors in Zn^{2+} resistance is promising for the overall study of metal resistance and homeostasis but outside the scope of this study.

Copper toxicity. (i) The Cus efflux system. The microbial response to Cu^{2+} toxicity has been well studied and was recently reviewed (1). However, our RB-TnSeq results reveal that few of the genes in the characterized copper export systems are essential to resistance in strain RCH2, while one uncharacterized gene, not previously associated with copper resistance, is essential. Some in the former category may still be used for copper resistance under other growth conditions or may not result in significant phenotypes due to genetic redundancy (such as the presence of a paralog); however, there were still surprisingly few genes predicted to be involved in copper resistance that had significantly negative fitness values.

Of the three RND-type transporter subunits encoded in the RCH2 genome, two contain CusA-type motifs (HME4), as defined by Nies (9), and are found in the associated region of the phylogenetic tree in Fig. S1 in the supplemental material. Thus, we will refer to the *cus* genes in the two associated operons as *cusC1B1A1F* (Psest_0598 to Psest_0595) and *cusC2B2A2* (Psest_2265 to Psest_2263) (Fig. 3). Psest_2262 is the last gene in the *cusC2* operon and is annotated in UniProt as "Co/Zn/Cd efflux system component." It is a member of the IPR002524 family of (mostly Zn^{2+}) efflux proteins that does not have a known association with the *cus* system. One might expect the *cusF*-containing *cusC1* operon to have a more-negative fitness value, since *cusF* has been shown in *E. coli* to improve copper resistance (15); however, of the two *cus* operons, only *cusC2B2A2* had w_{Cu} values of less than −1 (−1.9, −1.4, and −1.5, respectively), indicating that the *cusC2* operon is primarily used under these conditions (Fig. 3). In *E. coli*, CusF is a periplasmic Cu^{+} binding protein that delivers

Cu^+ to CusB for export (11, 13). In contrast with *E. coli*, however, the *cusB* genes in *P. stutzeri* RCH2 contain sequence homology that also places them in the CusF protein family (IPR021647) (60), indicating that this gene fusion may functionally replace a separate *cusF* gene to some extent in the *cusC2* operon. The existence of such gene fusions has been recognized previously (60). A total of 31% of sequenced CusF proteins (1,001 proteins) exist as fusions with RND-type efflux domains such as CusB (IPR032317) (see Fig. S3). Roughly a third of organisms that have such fusions lack separate *cusF* genes, further indicating that the fusion protein is able to replace the two acting independently, even though the fusion CusF domain will be less diffusible than a separate CusF. *P. stutzeri* RCH2 does not contain homologs of the regulatory genes *cusR* and *cusS* found in the *cus* locus in *E. coli*, and sequence analysis of upstream regions of both *cus* operons did not reveal putative regulatory sequences similar to the *E. coli* CusR box (61); thus, it is unclear how or whether the *cus* operons are regulated.

(ii) The Cue system. Strain RCH2 also contains homologs of the *cue* genes, *cueZ* and *cueAR* (Psest_0739 to Psest_0737), that were characterized in *E. coli* (62). Other *cueZ* and *cueA* homologs are also present, but not as adjacent genes (Fig. 3). No *cueO* homolog (63) is located adjacent to other *cue* genes. CueA is a Cu^+ P-type ATPase efflux pump, generally regulated by CueR (64), and CueZ is a Cu^+ binding protein (65). There was insufficient data to assign a confident fitness value for *cueZ*, and *cueAR* resulted in weak phenotypes (w_{Cu} values of −0.9 and −0.6) (Fig. 3) relative to the phenotype resulting from *cusA2*. This is in contrast to what is reported for *E. coli*, where the Cue system is dominant under both aerobic and anaerobic conditions (62). However, the CueA ATPase still appears to cooperate with the periplasmic Cus efflux system in strain RCH2, just as in anaerobically grown *E. coli*. The reduced severity of the phenotype resulting from *cueA* (called *copA* in reference 62) may indicate the presence of some other system that concomitantly exports copper across the plasma membrane in strain RCH2.

For CueR regulon reconstruction, the binding motif reported in *P. aeruginosa* (38) was refined by comparative analysis of regions upstream from *cueA* in *Pseudomonas* species *P. aeruginosa*, *P. fluorescens*, *P. entomophila*, *P. stutzeri*, *P. syringae*, and *P. putida*. In all cases except *P. aeruginosa*, *cueA* and *cueR* genes are cotranscribed, and thus, CueR-dependent regulation of the *cueAR* operon was expected. Indeed, a conserved 23-bp inverted repeat was identified (see Table S8 in the supplemental material), corresponding to the motif from *P. aeruginosa*. A search for the refined binding motif in *P. stutzeri* RCH2 (see Fig. S2) identified two putative CueR target genes in addition to the *cueAR* operon binding sites (see Table S8). The first of these genes is *cueZ*. The second is Psest_1595, which is likely cotranscribed with downstream genes Psest_1594 and Psest_1593. The Psest_1595 gene product belongs to COG2608, which also includes CueZ and other copper chaperones, but the gene did not exhibit a w_{Cu} value of less than −1. Thus, the observed phenotype resulting from *cueR* was likely caused by the lack of expression of *cueA*.

(iii) The Cop systems. RCH2 contains two sets of homologs to copper resistance *cop* genes that have been characterized primarily in *Pseudomonas syringae* (10). These are located at Psest_0581 (*copR1*), Psest_0583, Psest_0585, and Psest_0586 (*copA1B1M1*), Psest_1598 and Psest_1599 (*copR25*), Psest_1590, Psest_1588, and Psest_1587 (*copA2B2M2*), and Psest_3400 (*copD*). Both *copA* operons contain noncanonical genes (Psest_0582, Psest_0584, and Psest_1589). The only *cop* genes with w_{Cu} values of less than −0.6 were *copR1* (−1.2) and Psest_0584 (−0.9). *copM1* actually had positive fitness (w_{Cu} of 0.4) (Fig. 3). While this value is not very large, positive fitness values are rather unusual in these types of analysis, and *copM* has been previously reported to contribute to copper resistance in *Xanthomonas* species (7). The role of these cytochrome *c* proteins has yet to be elucidated, but it appears that they can either enhance or decrease copper resistance. In addition, the outer membrane protein CopB has been shown to enhance copper resistance in *P. syringae* and *Xanthomonas* species (7, 66) but has a minimal effect in strain RCH2. Psest_0584 is a hypothetical protein of 100 amino acids with homologs ($E < 10^{-5}$) found only in members of the *Pseudomonas* genus, and thus, it may represent a genus-specific copper resistance factor. Given the homology to copper resistance operons in *P. syringae* and *Xanthomonas*, it is surprising that the more widespread *copABM* genes had fitness values rather close to zero and that the most negative fitness value in these operons is from a gene encoding a hypothetical protein. Clearly, this system is not crucial to copper resistance in strain RCH2 under denitrifying conditions. This may be related to the fact that CopA, as a multicopper oxidase, is likely only active under aerobic conditions.

Interestingly, of the two CopR response regulators in strain RCH2, only *copR1*, which lacks the accompanying *copS* gene, had a w_{Cu} value of less than −1. Reconstruction of the CopRS regulon in *P. stutzeri* RCH2 demonstrated that both *copA* operons have predicted CopR binding sites in the upstream regions (see Table S8 and Fig. S2 in the supplemental material). CopR binding sites were also identified upstream from *copR1* and the *copR2S* operon, suggesting autoregulation, and upstream from Psest_0600, encoding a P-type ATPase transporter. A final CopR binding site was found upstream from the Psest_1595-to-Psest_1593 operon; thus, this operon is coregulated by two copper-responsive regulatory systems, CueR and CopRS. There is no striking difference between the CopR binding sites found upstream of *copR1* and *copR2* that could explain the different fitness values of the regulatory mutants. However, *copR1* is colocalized with the Psest_0582-to-Psest_0586 operon, which contains the only CopR target gene, Psest_0584, with a notably negative w_{Cu} value (−0.9) (Fig. 3). We hypothesize that the locally synthesized CopR1 is more important for activation of Psest_0582 to Psest_0586 than the more distantly synthesized CopR2. Finally, some predicted members of the CopR (or CueR) regulon may indeed be copper regulated but perform functions unrelated to copper, such as response to other toxic compounds that often co-occur with elevated copper concentrations, as has been reported previously in *P. aeruginosa* (67).

While additional studies of the regulation and the expression levels of the genes related to copper resistance would be needed to complete the picture of how strain RCH2 responds to and resists copper toxicity, the fitness values and regulatory analysis presented here provide several new insights. For example, while a high degree of functional redundancy might be expected from the high degree of genetic redundancy among copper resistance systems in strain RCH2, certain proteins, such as CusA2B2C2 and, to a lesser extent, CopR1, Psest_0584, and CueA, may be regarded as the "front line" of defense in that they are individually essential to effective copper resistance (Fig. 3). Since CusA1B1C1F is unable to replace CusA2B2C2, the former complex seems to have some func-

tion other than copper export or is downregulated by a regulatory mechanism that could not be recognized by the methods used here.

(iv) The Mrp Na^+/H^+ antiporter subunit. In addition to many genes that would be expected to be among the top transport-related genes required for growth in the presence of copper, there were several that bear no clear connection to copper that had very negative fitness values. In particular, Psest_2850, whose product is annotated as an Mrp Na^+/H^+ antiporter subunit, has among the most negative transport-related w_{Cu} values (−1.8) (Fig. 3b). This gene is in a predicted six-gene operon (Psest_2846 to Psest_2851) encoding six putative subunits of such an antiporter; however, only Psest_2850 results in a significant phenotype (for all of the other genes, the w_{Cu} value was more than −0.2). Hence, it seems unlikely that the complex as a whole performs some vital function under these conditions. Such complexes are known to facilitate the export of alkali metal monovalent cations, such as Li^+, Na^+, and K^+, but have also been proposed to serve other functions due to their large size and multisubunit composition (68), given that there are much simpler antiporters that perform the known functions of Mrp antiporters. Our data suggest that the c subunit of this particular antiporter may facilitate the export of Cu^+ either alone or in combination with the products of other genes (redundancy could eliminate single mutant phenotypes). Indeed, based on the stronger phenotype, the antiporter would be the primary means of Cu^+ efflux from the cytoplasm, and CueA-mediated efflux would be less critical (though the *cueA* paralog Psest_0600 could also reduce the effects of the *cueA* mutation). Such a proposal is in agreement with prior suggestions both that Mrp antiporters may have other unidentified substrates (68) and also that some alkali metal ion transporters may allow some passage of Cu^+ (62, 69). The latter has been discussed in terms of entry of Cu^+ into the cell under conditions of copper toxicity, and both proposals are without direct evidence for any specific examples. Indeed, Cu^+ export by an Mrp complex may take only subtle adjustment, as Li^+ and Cu^+ differ by only 1 pm in ionic radius (76 and 77 pm, respectively, for an effective ionic radius of a 6-coordinate ion). However, their ligand preferences and chemistry are very different, as Cu^+ is a redox-active soft acid and extremely thiophilic, whereas Li^+ is redox inactive, a hard acid, and oxophilic. Psest_2850 does contain five methionine residues, which could be used to select for Cu^+ transport, as in the Cus transporter (13).

(v) Molybdenum metabolism. As in all full denitrifiers, denitrifying growth of strain RCH2 begins with nitrate reduction, catalyzed by the molybdenum cofactor (Moco) in nitrate reductase (NarGHI). Nitrite is produced from this reaction and is subsequently reduced by nitrite reductase (NirS), nitric oxide reductase (NorBC), and nitrous oxide reductase (NosZ) to produce nitric oxide, nitrous oxide, and dinitrogen gas, respectively, although nitrate reduction can accept enough electrons to sustain growth in the absence of the other steps (24). Nitric oxide reductase, however, is required for the detoxification of nitric oxide even if nitric oxide is not needed for its electron-accepting potential (24). In addition to NirS, which is a heme-using cytochrome, there is a phylogenetically unrelated nitrite reductase, NirK, which uses copper for catalysis. RCH2 contains genes for both, but we have only observed negative fitness for NirS (24).

Surprisingly, the transporter genes with the most negative w_{Cu} values have nothing at all to do with copper transport but, rather, encode the well-known transporter for molybdate (MoO_4^{2-}), ModABC (w_{Cu} of −2.8 ± 0.3 for *modAB*) (Fig. 4). These data

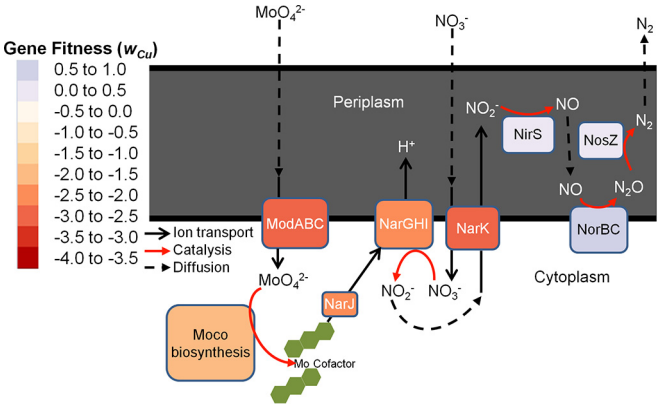

FIG 4 Copper sensitivities of denitrification-related mutants. Systems and genes involved in denitrification are color coded according to w_{Cu} values.

point to a major target for copper toxicity related to molybdenum. In agreement with this, there were negative w_{Cu} values for several genes involved in Moco biosynthesis (see Table S7 in the supplemental material) and nitrate reduction (w_{Cu} of −2.0 ± 0.3 for NarGHI) (Fig. 4). While enhanced demand for molybdenum may, to some extent, simply reflect greater energy demands on the cell due to the need to continuously remove Cu^+, we also measured w_{Cu} values of 0.4 ± 0.1 for *nirBCDEFJS* and 0.8 ± 0.3 for *norBCDQ* (Fig. 4). The decreased *nar* fitness combined with improved *nir* and *nor* fitness suggest that nitrite reductase may be inhibited by copper. In normal medium, *nar* mutants grown in the mutant pool can survive and grow to some extent by using nitrite released by other mutants in the pool. However, if copper inhibits Nir, this would no longer be an option, which would decrease the fitness values for genes involved in nitrate reduction, Moco biosynthesis, and MoO_4^{2-} uptake, as was observed. Mutations in *nir* and *nor* would no longer be detrimental because Nir is ineffective even when present, due to copper inhibition, and in the absence of properly functioning Nir, nitric oxide toxicity is reduced, so the disadvantage of *nor* mutations is also reduced. If this is true, it would mean that the use of the copper-dependent nitrite reductase would be favored over iron-dependent nitrite reductase under high copper conditions, as well as under iron-limited conditions. Finally, copper is highly thiophilic and has been reported to bind to the dithiolene moiety of pyranopterin (70), which could compete for molybdenum insertion, particularly under conditions of low intracellular MoO_4^{2-}, as in *modABC* mutants. This factor likely contributed to the negative w_{Cu} values observed for *modABC* but does not appear to have been a dominant effect, because the pattern of fitness values for *nir* and *nor* genes does not follow that of molybdenum limitation (24), a metabolic state similar to that of weak Moco biosynthesis.

Zinc toxicity: molybdenum metabolism. Zn^{2+} also caused negative fitness values for the nitrate reductase *narGHI* genes (w_{Zn} of −2.5 ± 0.2) and those involved in Moco biosynthesis (−3.2 ± 0.5, excluding *moaA1* and *-2*), and yet, the w_{Zn} values were less negative than the w_{Cu} values for the Mo transport *modABC* genes (−1.3 ± 0.0 for *modAB*) (Fig. 5). Zinc is less thiophilic than copper and, consequently, would be expected to cause less interference with molybdenum insertion into pyranopterin than was reported for copper (70), perhaps lowering the required intracellular MoO_4^{2-} concentration to that which can be satisfied by sul-

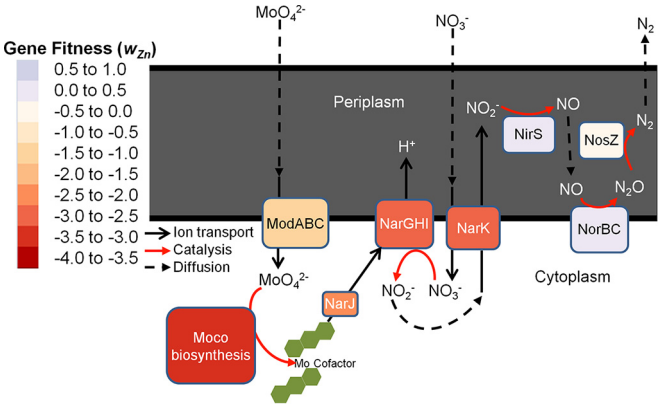

FIG 5 Zinc sensitivities of denitrification-related mutants. Systems and genes involved in denitrification are color coded according to w_{Zn} values.

fate and, possibly, other transporters (24). In addition, although the metal ion concentrations were chosen in an effort to achieve uniform growth defects for both toxic metals, the Zn^{2+}-supplemented growth was slower. Slower growth kinetics may enable the rate of MoO_4^{2-} uptake through the sulfate transporter to more closely match the Mo demands of the cell; however, increased energy demands and likely some inhibition of Nir combine to reduce Moco biosynthesis and *nar* mutant fitness and leave *nir* mutant fitness near zero in this case.

A revised perspective on copper and zinc toxicity. While Cu^{2+} and Zn^{2+} toxicity have been well studied in certain organisms, RB-TnSeq analysis in *Pseudomonas stutzeri* RCH2, a species with little previous characterization of metal resistance mechanisms, has shown that there are systems involved and impacts of elevated metal ion concentrations that are still unexplored. The well-known Zn^{2+} exporters CzcD and CzcCBA were identified from among other similar CDF- and RND-type transporter homologs, and phylogenetic analysis helped to more clearly delineate between *czcA* and *cusA* RND subfamilies. The CzcI component of this transporter has not been characterized like the rest of the CzcCBA transporter, but the w_{Zn} value of *czcI* was the most negative in the *czcICBA* operon, indicating that it is required for the proper function of this transporter in strain RCH2. A putative CzcR binding motif was identified and the corresponding regulon described, including Psest_0618. Psest_0618 mutant strains showed zinc sensitivity, implicating this hypothetical protein in zinc resistance. In addition, several other genes that had no previous connection with zinc toxicity exhibited w_{Zn} values of less than −1. Based on fitness values, cofitness, and previous characterization of mutants (53), we propose that CorB and CorC cooperate in metal ion efflux, including efflux of Mg^{2+} and Zn^{2+}, independently of the CorA Mg^{2+} transporter. Two annotated hypothetical proteins, Psest_3226 and Psest_3322, also had very high negative w_{Zn} fitness values. Psest_3226 is found across all three domains of life, including in humans, where a homolog was recently connected with a congenital glycosylation disorder (48). Our data extend the function of transporters in this family to Zn^{2+} efflux in the first report on a bacterial homolog. Psest_3322 and Psest_0618, on the other hand, are more restricted taxonomically, with no characterized homologs. The Zn^{2+} sensitivity of mutants lacking these genes gives a starting point for characterization of members of these uncharacterized protein families. Finally we constructed individual mutant strains with deletions of *czcI*, *corB*, *corC*, Psest_3226, and Psest_3322 and confirmed the resulting phenotypes shown by the RB-TnSeq data.

There are five predicted copper efflux systems in strain RCH2, but only two of them—one of the two *cusCBA* operons and the *cueA* gene—had w_{Cu} values of less than −0.9 for known transporter-encoding genes under anaerobic growth conditions. Curiously, the *cus* operon that lacks *cusF*, which has been implicated in Cu^{2+} efflux through CusCBA in *E. coli*, was the one with the more negative w_{Cu} value. The *cusB* genes, however, both contain *cusF* signatures. Thus, these CusB-CusF fusion proteins may be able to carry out both functions to some extent. No evidence of *cus* regulation could be identified using the methods reported here. The two *cop* operons, which are homologous to copper resistance operons in both *P. syringae* and *Xanthomonas* species, did not contain any known transporter-encoding genes with a w_{Cu} value more negative than −0.6; however, *copR1* and Psest_0584, a gene with unknown function, had w_{Cu} values of −1.2 and −0.9, respectively. Psest_0584 is not found outside the *Pseudomonas* genus but is likely to increase Cu^{2+} resistance among pseudomonads. Regulon reconstruction and analysis for CueR and CopR yielded a refined CueR binding motif and identified several regulon members outside the recognized copper transport operons, including the coregulated Psest_1595-to-Psest_1593 operon, but none with negative w_{Cu} values. Lastly, a subunit of an Mrp-type Na^+/H^+ antiporter had an unexpectedly negative w_{Cu} value of −1.8. We suggest that this subunit may allow this antiporter to transport Cu^+. This is in accord with the suggestion that Mrp antiporters perform more functions than have been characterized so far, which would justify their size and complexity relative to those of other classes of Na^+/H^+ antiporters (68).

Cu^{2+} and Zn^{2+} induced decreases in fitness values for several genes involved in denitrification, Moco biosynthesis, and molybdenum uptake (Fig. 4 and 5). Some of these effects may be due to the increased energetic demands on the cell to continuously pump out metal ions; however, the pattern of fitness values was not simply an amplification of what is seen under typical denitrifying conditions. Instead, particularly for Cu^{2+}, the fitness values for *nar* genes, as well as those involved in Moco biosynthesis and molybdenum uptake, decreased, while the values for *nir* and *nor* genes increased. Nitric oxide reduction, which is facilitated by the Nor system, is needed for detoxification of nitric oxide during denitrifying growth, so these changes indicate a reduced rate of nitric oxide production, which is consistent with copper inhibition of NirS, the active nitrite reductase. The fitness values for *modABC*, encoding the MoO_4^{2-} ABC transporter, were very negative, which could be a sign of copper interference with molybdenum insertion into pyranopterin. The pattern of fitness values was similar under conditions of Zn^{2+} toxicity, except that the fitness values for *modABC* were closer to those for the control and the fitness values for Moco biosynthesis genes were much more negative. We hypothesize that zinc toxicity caused a similar inhibition of NirS, but the combination of a lower growth rate and the absence of significant competition for the pyranopterin dithiolene relaxed the requirement for functioning ModABC and emphasized the effect of a lack in any of the Moco biosynthesis genes. In summary, we both extend the number of genes known to be involved in zinc and copper efflux and resistance and expand the understanding of important intracellular targets for metal binding and toxicity.

ACKNOWLEDGMENTS

We thank Morgan N. Price for assistance in data processing and Farris L. Poole, Jr., for helpful discussion concerning bioinformatic analysis.

FUNDING INFORMATION

This work, including the efforts of Brian J. Vaccaro, William A. Lancaster, Michael P. Thorgersen, Grant Zane, Adam D. Younkin, Alexey E. Kazakov, Kelly M. Wetmore, Adam Deutschbauer, Adam P. Arkin, Pavel Novichkov, Judy D. Wall, and Michael W. W. Adams, was funded by Department of Energy, Office of Science (DE-AC02-05CH11231).

This material by ENIGMA (Ecosystems and Networks Integrated with Genes and Molecular Assemblies; http://enigma.lbl.gov), a Scientific Focus Area Program at Lawrence Berkeley National Laboratory, is based upon work supported by the U.S. Department of Energy, Office of Science, Office of Biological & Environmental Research, under contract number DE-AC02-05CH11231.

REFERENCES

1. **Braymer JJ, Giedroc DP.** 2014. Recent developments in copper and zinc homeostasis in bacterial pathogens. Curr Opin Chem Biol **19:**59–66. http://dx.doi.org/10.1016/j.cbpa.2013.12.021.
2. **Sawyer DT, Sobkowiak A, Matsushita T.** 1996. Metal [ML_x; M = Fe, Cu, Co, Mn]/hydroperoxide-induced activation of dioxygen for the oxygenation of hydrocarbons: oxygenated Fenton chemistry. Acc Chem Res **29:**409–416. http://dx.doi.org/10.1021/ar950031c.
3. **Macomber L, Imlay JA.** 2009. The iron-sulfur clusters of dehydratases are primary intracellular targets of copper toxicity. Proc Natl Acad Sci U S A **106:**8344–8349. http://dx.doi.org/10.1073/pnas.0812808106.
4. **Crisponi G, Nurchi VM, Fanni D, Gerosa C, Nemolato S, Faa G.** 2010. Copper-related diseases: from chemistry to molecular pathology. Coord Chem Rev **254:**876–889. http://dx.doi.org/10.1016/j.ccr.2009.12.018.
5. **Kury S, Dreno B, Bezieau S, Giraudet S, Kharfi M, Kamoun R, Moisan J-P.** 2002. Identification of SLC39A4, a gene involved in acrodermatitis enteropathica. Nat Genet **31:**239–240. http://dx.doi.org/10.1038/ng913.
6. **Kozlowski H, Luczkowski M, Remelli M, Valensin D.** 2012. Copper, zinc and iron in neurodegenerative diseases (Alzheimer's, Parkinson's and prion diseases). Coord Chem Rev **256:**2129–2141. http://dx.doi.org/10.1016/j.ccr.2012.03.013.
7. **Behlau F, Canteros BI, Minsavage GV, Jones JB, Graham JH.** 2011. Molecular characterization of copper resistance genes from *Xanthomonas citri* subsp. *citri* and *Xanthomonas alfalfae* subsp. *citrumelonis*. Appl Environ Microbiol **77:**4089–4096. http://dx.doi.org/10.1128/AEM.03043-10.
8. **Inesi G, Pilankatta R, Tadini-Buoninsegni F.** 2014. Biochemical characterization of P-type copper ATPases. Biochem J **463:**167–176. http://dx.doi.org/10.1042/BJ20140741.
9. **Nies DH.** 2003. Efflux-mediated heavy metal resistance in prokaryotes. FEMS Microbiol Rev **27:**313–339. http://dx.doi.org/10.1016/S0168-6445(03)00048-2.
10. **Cooksey DA.** 1994. Molecular mechanisms of copper resistance and accumulation in bacteria. FEMS Microbiol Rev **14:**381–386. http://dx.doi.org/10.1111/j.1574-6976.1994.tb00112.x.
11. **Kim E-H, Nies DH, McEvoy MM, Rensing C.** 2011. Switch or funnel: how RND-type transport systems control periplasmic metal homeostasis. J Bacteriol **193:**2381–2387. http://dx.doi.org/10.1128/JB.01323-10.
12. **Anton A, Große C, Reißmann J, Pribyl T, Nies DH.** 1999. CzcD is a heavy metal ion transporter involved in regulation of heavy metal resistance in *Ralstonia* sp. strain CH34. J Bacteriol **181:**6876–6881.
13. **Delmar JA, Su C-C, Yu EW.** 2013. Structural mechanisms of heavy-metal extrusion by the Cus efflux system. Biometals **26:**593–607. http://dx.doi.org/10.1007/s10534-013-9628-0.
14. **von Rozycki T, Nies DH.** 2009. *Cupriavidus metallidurans*: evolution of a metal-resistant bacterium. Antonie Van Leeuwenhoek **96:**115–139. http://dx.doi.org/10.1007/s10482-008-9284-5.
15. **Franke S, Grass G, Rensing C, Nies DH.** 2003. Molecular analysis of the copper-transporting efflux system CusCFBA of *Escherichia coli*. J Bacteriol **185:**3804–3812. http://dx.doi.org/10.1128/JB.185.13.3804-3812.2003.
16. **Long F, Su C-C, Zimmermann MT, Boyken SE, Rajashankar KR, Jernigan RL, Yu EW.** 2010. Crystal structures of the CusA efflux pump suggest methionine-mediated metal transport. Nature **467:**484–488. http://dx.doi.org/10.1038/nature09395.
17. **Allen Gregory S, Wu C-C, Cardozo T, Stokes DL.** 2011. The architecture of CopA from *Archeaoglobus fulgidus* studied by cryo-electron microscopy and computational docking. Structure **19:**1219–1232. http://dx.doi.org/10.1016/j.str.2011.05.014.
18. **Lu M, Fu D.** 2007. Structure of the zinc transporter YiiP. Science **317:**1746–1748. http://dx.doi.org/10.1126/science.1143748.
19. **Nies DH, Nies A, Chu L, Silver S.** 1989. Expression and nucleotide sequence of a plasmid-determined divalent cation efflux system from *Alcaligenes eutrophus*. Proc Natl Acad Sci U S A **86:**7351–7355. http://dx.doi.org/10.1073/pnas.86.19.7351.
20. **Moore CM, Gaballa A, Hui M, Ye RW, Helmann JD.** 2005. Genetic and physiological responses of *Bacillus subtilis* to metal ion stress. Mol Microbiol **57:**27–40. http://dx.doi.org/10.1111/j.1365-2958.2005.04642.x.
21. **Kloosterman TG, Van Der Kooi-Pol MM, Bijlsma JJE, Kuipers OP.** 2007. The novel transcriptional regulator SczA mediates protection against Zn^{2+} stress by activation of the Zn^{2+}-resistance gene *czcD* in *Streptococcus pneumoniae*. Mol Microbiol **65:**1049–1063. http://dx.doi.org/10.1111/j.1365-2958.2007.05849.x.
22. **van der Lelie D, Schwuchow T, Schwidetzky U, Wuertz S, Baeyens W, Mergeay M, Nies DH.** 1997. Two-component regulatory system involved in transcriptional control of heavy-metal homoeostasis in *Alcaligenes eutrophus*. Mol Microbiol **23:**493–503. http://dx.doi.org/10.1046/j.1365-2958.1997.d01-1866.x.
23. **Niegowski D, Eshaghi S.** 2007. The CorA family: structure and function revisited. Cell Mol Life Sci **64:**2564–2574. http://dx.doi.org/10.1007/s00018-007-7174-z.
24. **Vaccaro BJ, Thorgersen MP, Lancaster WA, Price MN, Wetmore KM, Poole FL, Deutschbauer A, Arkin AP, Adams MWW.** 2016. Determining roles of accessory genes in denitrification by mutant fitness analyses. Appl Environ Microbiol **82:**51–61. http://dx.doi.org/10.1128/AEM.02602-15.
25. **Gisin J, Müller A, Pfänder Y, Leimkühler S, Narberhaus F, Masepohl B.** 2010. A *Rhodobacter capsulatus* member of a universal permease family imports molybdate and other oxyanions. J Bacteriol **192:**5943–5952. http://dx.doi.org/10.1128/JB.00742-10.
26. **Mitchell A, Chang HY, Daugherty L, Fraser M, Hunter S, Lopez R, McAnulla C, McMenamin C, Nuka G, Pesseat S, Sangrador-Vegas A, Scheremetjew M, Rato C, Yong SY, Bateman A, Punta M, Attwood TK, Sigrist CJ, Redaschi N, Rivoire C, Xenarios I, Kahn D, Guyot D, Bork P, Letunic I, Gough J, Oates M, Haft D, Huang H, Natale DA, Wu CH, Orengo C, Sillitoe I, Mi H, Thomas PD, Finn RD.** 2015. The InterPro protein families database: the classification resource after 15 years. Nucleic Acids Res **43:**D213–D221. http://dx.doi.org/10.1093/nar/gku1243.
27. **Macomber L, Rensing C, Imlay JA.** 2007. Intracellular copper does not catalyze the formation of oxidative DNA damage in *Escherichia coli*. J Bacteriol **189:**1616–1626. http://dx.doi.org/10.1128/JB.01357-06.
28. **Lalucat J, Bennasar A, Bosch R, García-Valdés E, Palleroni NJ.** 2006. Biology of *Pseudomonas stutzeri*. Microbiol Mol Biol Rev **70:**510–547. http://dx.doi.org/10.1128/MMBR.00047-05.
29. **Han R, Geller JT, Yang L, Brodie EL, Chakraborty R, Larsen JT, Beller HR.** 2010. Physiological and transcriptional studies of Cr(VI) reduction under aerobic and denitrifying conditions by an aquifer-derived pseudomonad. Environ Sci Technol **44:**7491–7497. http://dx.doi.org/10.1021/es101152r.
30. **Wetmore KM, Price MN, Waters RJ, Lamson JS, He J, Hoover CA, Blow MJ, Bristow J, Butland G, Arkin AP, Deutschbauer A.** 2015. Rapid quantification of mutant fitness in diverse bacteria by sequencing randomly bar-coded transposons. mBio **6:**e00306-15. http://dx.doi.org/10.1128/mBio.00306-15.
31. **Widdel F, Bak F.** 1992. Gram-negative mesophilic sulfate-reducing bacteria, p 3352–3378. *In* Balows A, Trüper H, Dworkin M, Harder W, Schleifer K-H (ed), The prokaryotes. Springer, New York, NY. http://dx.doi.org/10.1007/978-1-4757-2191-1_21.
32. **Li MZ, Elledge SJ.** 2007. Harnessing homologous recombination in vitro to generate recombinant DNA via SLIC. Nat Methods **4:**251–256. http://dx.doi.org/10.1038/nmeth1010.
33. **Horton RM, Cai ZL, Ho SN, Pease LR.** 1990. Gene splicing by overlap extension: tailor-made genes using the polymerase chain reaction. Biotechniques **8:**528–535.
34. **Larsen RA, Wilson MM, Guss AM, Metcalf WW.** 2002. Genetic analysis of pigment biosynthesis in *Xanthobacter autotrophicus* Py2 using a new, highly efficient transposon mutagenesis system that is functional in a wide variety of bacteria. Arch Microbiol **178:**193–201. http://dx.doi.org/10.1007/s00203-002-0442-2.
35. **Fels SR, Zane GM, Blake SM, Wall JD.** 2013. Rapid transposon liquid

enrichment sequencing (TnLE-seq) for gene fitness evaluation in underdeveloped bacterial systems. Appl Environ Microbiol **79:**7510–7517. http://dx.doi.org/10.1128/AEM.02051-13.
36. **Zane GM, Yen HC, Wall JD.** 2010. Effect of the deletion of *qmoABC* and the promoter-distal gene encoding a hypothetical protein on sulfate reduction in *Desulfovibrio vulgaris* Hildenborough. Appl Environ Microbiol **76:**5500–5509. http://dx.doi.org/10.1128/AEM.00691-10.
37. **Perron K, Caille O, Rossier C, van Delden C, Dumas J-L, Köhler T.** 2004. CzcR-CzcS, a two-component system involved in heavy metal and carbapenem resistance in *Pseudomonas aeruginosa*. J Biol Chem **279:**8761–8768. http://dx.doi.org/10.1074/jbc.M312080200.
38. **Thaden JT, Lory S, Gardner TS.** 2010. Quorum-sensing regulation of a copper toxicity system in *Pseudomonas aeruginosa*. J Bacteriol **192:**2557–2568. http://dx.doi.org/10.1128/JB.01528-09.
39. **Mills SD, Lim CK, Cooksey DA.** 1994. Purification and characterization of CopR, a transcriptional activator protein that binds to a conserved domain (cop box) in copper-inducible promoters of *Pseudomonas syringae*. Mol Gen Genet **244:**341–351.
40. **Novichkov PS, Rodionov DA, Stavrovskaya ED, Novichkova ES, Kazakov AE, Gelfand MS, Arkin AP, Mironov AA, Dubchak I.** 2010. RegPredict: an integrated system for regulon inference in prokaryotes by comparative genomics approach. Nucleic Acids Res **38:**W299–W307. http://dx.doi.org/10.1093/nar/gkq531.
41. **Mironov AA, Vinokurova NP, Gelfand MS.** 2000. Software for analysis of bacterial genomes. Mol Biol **34:**222–231. http://dx.doi.org/10.1007/BF02759643.
42. **van Opijnen T, Bodi KL, Camilli A.** 2009. Tn-seq: high-throughput parallel sequencing for fitness and genetic interaction studies in microorganisms. Nat Methods **6:**767–772. http://dx.doi.org/10.1038/nmeth.1377.
43. **Scherer J, Nies DH.** 2009. CzcP is a novel efflux system contributing to transition metal resistance in *Cupriavidus metallidurans* CH34. Mol Microbiol **73:**601–621. http://dx.doi.org/10.1111/j.1365-2958.2009.06792.x.
44. **UniProt Consortium.** 2015. UniProt: a hub for protein information. Nucleic Acids Res **43:**D204–D212. http://dx.doi.org/10.1093/nar/gku989.
45. **de Castro E, Sigrist CJA, Gattiker A, Bulliard V, Langendijk-Genevaux PS, Gasteiger E, Bairoch A, Hulo N.** 2006. ScanProsite: detection of PROSITE signature matches and ProRule-associated functional and structural residues in proteins. Nucleic Acids Res **34:**W362–W365. http://dx.doi.org/10.1093/nar/gkl124.
46. **Grosse C, Grass G, Anton A, Franke S, Santos AN, Lawley B, Brown NL, Nies DH.** 1999. Transcriptional organization of the *czc* heavy-metal homeostasis determinant from *Alcaligenes eutrophus*. J Bacteriol **181:**2385–2393.
47. **Xiong J, Li D, Li H, He M, Miller SJ, Yu L, Rensing C, Wang G.** 2011. Genome analysis and characterization of zinc efflux systems of a highly zinc-resistant bacterium, Comamonas testosteroni S44. Res Microbiol **162:**671–679. http://dx.doi.org/10.1016/j.resmic.2011.06.002.
48. **Foulquier F, Amyere M, Jaeken J, Zeevaert R, Schollen E, Race V, Bammens R, Morelle W, Rosnoblet C, Legrand D, Demaegd D, Buist N, Cheillan D, Guffon N, Morsomme P, Annaert W, Freeze HH, Van Schaftingen E, Vikkula M, Matthijs G.** 2012. TMEM165 deficiency causes a congenital disorder of glycosylation. Am J Hum Genet **91:**15–26. http://dx.doi.org/10.1016/j.ajhg.2012.05.002.
49. **Demaegd D, Foulquier F, Colinet A-S, Gremillon L, Legrand D, Mariot P, Peiter E, Van Schaftingen E, Matthijs G, Morsomme P.** 2013. Newly characterized Golgi-localized family of proteins is involved in calcium and pH homeostasis in yeast and human cells. Proc Natl Acad Sci U S A **110:**6859–6864. http://dx.doi.org/10.1073/pnas.1219871110.
50. **Demaegd D, Colinet A-S, Deschamps A, Morsomme P.** 2014. Molecular evolution of a novel family of putative calcium transporters. PLoS One **9:**e100851. http://dx.doi.org/10.1371/journal.pone.0100851.
51. **Finn RD, Coggill P, Eberhardt RY, Eddy SR, Mistry J, Mitchell AL, Potter SC, Punta M, Qureshi M, Sangrador-Vegas A, Salazar GA, Tate J, Bateman A.** 2016. The Pfam protein families database: towards a more sustainable future. Nucleic Acids Res **44:**D279–D285. http://dx.doi.org/10.1093/nar/gkv1344.
52. **Sigrist CJA, de Castro E, Cerutti L, Cuche BA, Hulo N, Bridge A, Bougueleret L, Xenarios I.** 2013. New and continuing developments at PROSITE. Nucleic Acids Res **41**(Database issue):D344–D347. http://dx.doi.org/10.1093/nar/gks1067.
53. **Gibson MM, Bagga DA, Miller CG, Maguire ME.** 1991. Magnesium transport in *Salmonella typhimurium*: the influence of new mutations conferring Co^{2+} resistance on the CorA Mg^{2+} transport system. Mol Microbiol **5:**2753–2762. http://dx.doi.org/10.1111/j.1365-2958.1991.tb01984.x.
54. **Papp-Wallace K, Maguire M.** 25 September 2008. Magnesium transport and magnesium homeostasis. EcoSal Plus 2008 http://dx.doi.org/10.1128/ecosalplus.5.4.4.2.
55. **Deutschbauer A, Price MN, Wetmore KM, Tarjan DR, Xu Z, Shao W, Leon D, Arkin AP, Skerker JM.** 2014. Towards an informative mutant phenotype for every bacterial gene. J Bacteriol **196:**3643–3655. http://dx.doi.org/10.1128/JB.01836-14.
56. **Hillenmeyer ME, Fung E, Wildenhain J, Pierce SE, Hoon S, Lee W, Proctor M, St Onge RP, Tyers M, Koller D, Altman RB, Davis RW, Nislow C, Giaever G.** 2008. The chemical genomic portrait of yeast: uncovering a phenotype for all genes. Science **320:**362–365. http://dx.doi.org/10.1126/science.1150021.
57. **Kasten U, Mullenders LHF, Hartwig A.** 1997. Cobalt(II) inhibits the incision and the polymerization step of nucleotide excision repair in human fibroblasts. Mutat Res **383:**81–89. http://dx.doi.org/10.1016/S0921-8777(96)00052-3.
58. **Snavely MD, Florer JB, Miller CG, Maguire ME.** 1989. Magnesium transport in *Salmonella typhimurium*: $^{28}Mg^{2+}$ transport by the CorA, MgtA, and MgtB systems. J Bacteriol **171:**4761–4766.
59. **Papp-Wallace KM, Maguire ME.** 2008. Regulation of CorA Mg^{2+} channel function affects the virulence of *Salmonella enterica* serovar Typhimurium. J Bacteriol **190:**6509–6516. http://dx.doi.org/10.1128/JB.00144-08.
60. **Kim E-H, Rensing C, McEvoy MM.** 2010. Chaperone-mediated copper handling in the periplasm. Nat Prod Rep **27:**711–719. http://dx.doi.org/10.1039/b906681k.
61. **Urano H, Umezawa Y, Yamamoto K, Ishihama A, Ogasawara H.** 2015. Cooperative regulation of the common target genes between H_2O_2-sensing YedVW and Cu^{2+}-sensing CusSR in *Escherichia coli*. Microbiology **161:**729–738. http://dx.doi.org/10.1099/mic.0.000026.
62. **Outten FW, Huffman DL, Hale JA, O'Halloran TV.** 2001. The independent *cue* and *cus* systems confer copper tolerance during aerobic and anaerobic growth in *Escherichia coli*. J Biol Chem **276:**30670–30677. http://dx.doi.org/10.1074/jbc.M104122200.
63. **Singh SK, Grass G, Rensing C, Montfort WR.** 2004. Cuprous oxidase activity of CueO from *Escherichia coli*. J Bacteriol **186:**7815–7817. http://dx.doi.org/10.1128/JB.186.22.7815-7817.2004.
64. **Outten FW, Outten CE, Hale J, O'Halloran TV.** 2000. Transcriptional activation of an *Escherichia coli* copper efflux regulon by the chromosomal MerR homologue, CueR. J Biol Chem **275:**31024–31029. http://dx.doi.org/10.1074/jbc.M006508200.
65. **Zhang X-X, Rainey PB.** 2008. Regulation of copper homeostasis in *Pseudomonas fluorescens* SBW25. Environ Microbiol **10:**3284–3294. http://dx.doi.org/10.1111/j.1462-2920.2008.01720.x.
66. **Puig S, Rees EM, Thiele DJ.** 2002. The ABCDs of periplasmic copper trafficking. Structure **10:**1292–1295. http://dx.doi.org/10.1016/S0969-2126(02)00863-8.
67. **Caille O, Rossier C, Perron K.** 2007. A copper-activated two-component system interacts with zinc and imipenem resistance in *Pseudomonas aeruginosa*. J Bacteriol **189:**4561–4568. http://dx.doi.org/10.1128/JB.00095-07.
68. **Swartz TH, Ikewada S, Ishikawa O, Ito M, Krulwich TA.** 2005. The Mrp system: a giant among monovalent cation/proton antiporters? Extremophiles **9:**345–354. http://dx.doi.org/10.1007/s00792-005-0451-6.
69. **Große C, Schleuder G, Schmole C, Nies DH.** 2014. Survival of *Escherichia coli* cells on solid copper surfaces is increased by glutathione. Appl Environ Microbiol **80:**7071–7078. http://dx.doi.org/10.1128/AEM.02842-14.
70. **Neumann M, Leimkühler S.** 2008. Heavy metal ions inhibit molybdoenzyme activity by binding to the dithiolene moiety of molybdopterin in *Escherichia coli*. FEBS J **275:**5678–5689. http://dx.doi.org/10.1111/j.1742-4658.2008.06694.x.